Residual Stress Assessment of PWMT Butt Joint with 10mm HSLA S460G2+M Steel using HFMI/PIT FEA and XRD

Noridzwan Nordin[1,*], *Muhd. Faiz* Mat[1], *Yupiter* H. P. Manurung[1], *Salina* Saidin[2], and *Dahia* Andud[3]

[1]Faculty of Mechanical Engineering, Universiti Teknologi MARA (UiTM) Shah Alam, Selangor, Malaysia
[2]Universiti Kuala Lumpur Malaysia France Institute, Selangor, Malaysia
[3]Nusantara Technologies Sdn, Bhd., Selangor, Malaysia

Abstract. This research involves the assessment of the residual stress of HSLA S460G2+M steel on butt joints which were welded using manual GMAW and further treated with HFMI/PIT process. The assessment began by manually welding 3-pass butt joint specimens using GMAW with ER80S-N1 as filler wire and mixed shielding gas (80%Ar-20%CO2). The weld toe of the specimens was then treated using HFMI/PIT operating at a peening frequency of 90Hz and a pneumatic pressure of 6 bar. The residual stress on the surface of treated and untreated specimens were measured using the X-ray diffraction method. Following the measurements, a simulation was conducted using non-linear solver FEA software MSC Marc/Mentat. The HFMI/PIT treatment process was simulated using a quasi-dynamic model approach for the force of the hammering pin. A customized spring function applying a consistent force onto the surface of the weld joint was modelled with this method. The material behavior model used for the specimen was based on a simplified Hensel-Spittel model obtained from the material database software MatILDa. It is observed that the HFMI/PIT-treated specimens induces compressive residual stress on the weld toe that is beneficial for fatigue life and the simulation demonstrated good agreement with the actual process.

1 Introduction

Use High Strength Low Alloy (HSLA) steel is a group of low-alloy, low-carbon steel in which the high yield strength is obtained through a thermomechanical controlled process (TMCP) during manufacturing. They are widely used in structures such as bridges, buildings, offshore platforms and heavy machineries [1]. S460 steel denotes that it is to be used for structural fabrication and have a nominal yield strength of 460MPa. S460 group of steel contains between 0.07% to 0.12% carbon, up to 2% manganese and the addition of niobium, vanadium and titanium in various amounts. These microalloying elements allow HSLA to achieve smaller grain size and precipitation hardening through controlled cooling and rolling process. The result is that HSLA steel have better corrosion resistance and yield strength than regular low carbon steel, but still maintain the same weldability as the latter [2].

S460G2+M is used extensively in large structural fabrication of offshore oil platform due to its high impact toughness in extreme cold weather. Table 1 and Table 2 below describe the mechanical properties and chemical composition of S460G2+M steel:

Table 1. Mechanical properties of S460G2+M steel [3].

Thickness	< 16mm
Yield strength	460 MPa (min)
Tensile Strength	540/700 MPa
Impact Energy	60J at -40°C
Elongation A %	17%

Table 2. Main chemical composition of S460G2+M steel (%) [3].

C	Si	Mn	Cr	Mo	Ni	Cu	Nb	V
0.14	0.15	1.65	0.25	0.25	0.7	0.3	0.04	0.08

Due to the way HSLA steel is manufactured, different parameters are required for its welding process compared to those usually used for low carbon steel. HSLA steel is also more sensitive to excessive temperature near its recrystallization point and requires a more controlled preheat and interpass heating than usual to preserve the finer grain structure that produced its high strength. Necessary care must also be given in

* Corresponding author: noridzwan.nordin@yahoo.com

matching the weld filler to the base metal to minimize heat-affected zone (HAZ) softening and to avoid hydrogen-induced cold cracking (HCC) [4]. Similarly, post-weld heat treatment (PWHT) usually used to reduce residual stress and distortion in welding joints is generally avoided for HSLA steel. If indeed necessary, the PWHT temperature used for such treatment is lower than is normally considered for low carbon steel [5].

2 Post-weld mechanical treatment using HFMI/PIT

An area of concern and ongoing research for HSLA welded joints is fatigue induced crack due to fluctuating load stress. Welded joints are most susceptible to fatigue induced crack due to their sharp geometric profile and the tensile residual stress formed by the welding process. Post-weld mechanical treatment (PWMT) is seen as a viable alternative to, and in many cases, even a beneficial addition to PWHT. While PWMT is not new, better techniques and methods have been developed that produces better and more consistent result than traditional methods.

The sharp geometric profile of the welding joints is traditionally minimized by either grinding, "dressing" the weld toe using Tungsten Inert Gas (TIG) to create a more rounded joint, or by peening with an air hammer. Newer methods to improve fatigue strength of welded joints is by mechanical peening techniques such as High Frequency Impact Treatment (HFMI) that improve the geometric profile of the welding joint while at the same time introduces compressive residual stress on the surface of the joint that would improve its fatigue strength [6]. Various implementations of the HFMI concept include Ultrasonic Impact Treatment (UIT), Ultrasonic Needle Peening (UNP), High Frequency Impact Treatment (HiFiT) and Pneumatic Impact Treatment (PIT) among others. Figure 1 shows the equipment used for HFMI/PIT treatment.

Fig. 1. Equipment used for HFMI/PIT treatment [7].

An advantage that HFMI/PIT has over traditional hammer peening is that it produced a more consistent result from the treatment of the weld joints. For example, the fluidic muscle system employed in HFMI/PIT method allows it to apply a consistent peening force onto the working surface and creates a more consistent rounding of the weld toe notch. This method also produces much lower vibrations than the regular air hammer, as low as $5ms^{-2}$, which would allow the operator to work continuously for up to 8 hours. The actuator of the hammering gun operates at a low voltage of 24V which allows it to be deployed underwater in a safe manner.

In the fabrication of welded structures, the design of welded joints using HSLA steel together with the need to account for its fatigue life is further complicated by the fact that the TMCP process used in its production introduces a non-linear residual stress along the thickness of the material. Steel plates produced by this rolling process, such as the S460 steel, typically produce a compressive residual near the surface of the plate that gradually transition into tensile residual stress towards the center [8]. This residual stress profile needs to be accounted for particularly when calculating the fatigue life using Finite Element Analysis (FEA) based method such as the Effective Notch Stress method.

3 Residual stress assessment of welded butt joint using XRD

The butt joint welded plates used in this research have a dimension of 300mm x 180mm x10mm with a V-groove angle of 60°, root gap of 2.5mm and root face of 2mm. The butt joint was manually welded using 3-pass Gas Metal Arc Welding (GMAW) with ER80S-Ni1 used as the filler wire. The shielding gas used was a mixture of 80% argon and 20% carbon dioxide. The choice of filler wire and shielding gas used was on consultation with the steel manufacturer. Both sides of the welding specimen plates were clamped on to the table during the welding process and removed after the specimens were cooled in air to room temperature to minimize welding distortion.

Several specimens were welded with different voltage and amperage settings to find the optimum welding parameters. The specimens were then machined into testing coupons and then ran through a series of tests to ascertain the quality of the weld joints. The tests were made according to American Welding Society (AWS) D1.1 standard for Welding Procedure Specification (WPS) qualification, which include tensile, bending, hardness and impact toughness testing. The specimen with the best test results was selected for further treatment with HFMI/PIT.

The HFMI/PIT equipment was set at an operating pressure of 6 bar and peening frequency of 90Hz as recommended by the equipment manufacturer. The hammering pin was positioned normal to the face of the weld toe at around 60° to the surface of the plate specimen. The peening was applied along one side of the weldment in multiple passes until an acceptably smooth notch was formed on the weld toe. A pin with a diameter of 4mm was used for peening as the angle of the weld toe was quite low and requires a wider notch radius.

The treated specimens were machined down to a smaller size to fit into the holding tray of the X-ray diffractometer (XRD). The bottom of the specimens was milled until their thickness were down to 5mm and the sides of the weldment were cut to an overall length of around 10mm. Then the specimens were chemically

cleaned in a phosphoric acid solution to remove any surface contamination and expose the bare metal surface. Three points on each side of the untreated and HFMI/PIT treated weld toes were arbitrarily selected for the residual stress measurements.

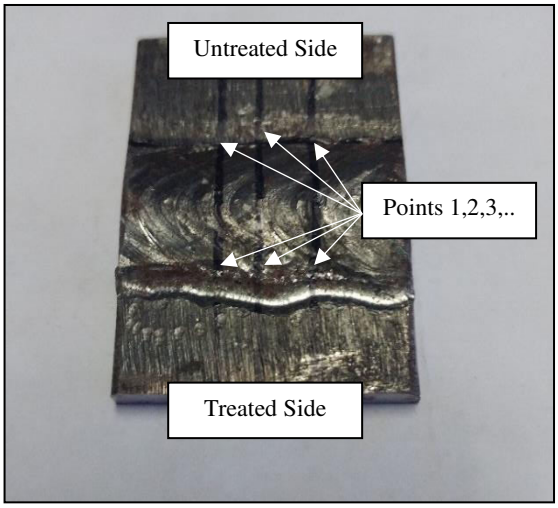

Fig. 2. Specimen used for the residual stress measurement.

The psi-tilting sin2Ψ method was used for the residual stress measurement. The XRD used a Cu-Kα radiation beam at 1600W (40kV, 40mA) with a tilting specimen holder that allowed measurements along the psi angle. The 2θ angle used was 138° with the psi angles measured in 5 steps of between 20° to 45°. The three points selected on both sides of the weld toes of the specimens were measured in longitudinal and transverse direction to the weld line. The rough texture of the surface tends to cause higher scattering due to the existence of shear residual stress from the peening process.

The measurements were taken in Fixed Time mode of 15 seconds per step at a step angle of 0.5° and total sweep angle of 3°. For measurements of the peened surface, the specimens were oscillated at 0.5° psi angle with an angular speed of 20°/min to improve the measurement quality. The residual stresses in the direction of the psi tilt were derived by linear regression of the plot of the 2θ against sin2Ψ values for each point on the specimen. To improve the accuracy of the residual stress calculation, an unstressed 2θ value of the specimens was obtained from a normalized sample that had been heat treated at 900°C for 1 hour and then cooled in open air down to room temperature. The 2θ value was used to determine the stress constant K that was used to calculate the residual stress of the measurements.

The stress (σ) and margin of error (Δσ) were calculated by multiplying the slope of the regression line M with the stress constant K using the following equation:

$$\sigma \pm \Delta\sigma = K(M \mp \Delta M) \quad (1)$$

where

$$K = -\frac{1}{2} \times \frac{E}{1+\nu} \times \cot\theta_0 \times \frac{\pi}{180} \quad (2)$$

$$M = \frac{\sum(X_i Y_i) - n\bar{X}\bar{Y}}{\sum {X_i}^2 - n\bar{X}^2} \quad (3)$$

$$\Delta M = t(n-2,\alpha) * \sqrt{\frac{\sum\{Y_i - (A+MX_i)\}^2}{(n-2)*\sum(X_i - \bar{X})^2}} \quad (4)$$

and

$$X_i = sin^2\Psi_i \quad (5)$$

$$Y_i = 2\theta_{\Psi ix} \quad (6)$$

$$\bar{X} = \frac{1}{n}\sum_{i=1}^{n} X_i \quad (7)$$

$$\bar{Y} = \frac{1}{n}\sum_{i=1}^{n} Y_i \quad (8)$$

$$A = \bar{Y} - M\bar{X} \quad (9)$$

4 Simulation of HFMI/PIT treatment on welded butt joint

The mesh modelling and simulation of the HFMI/PIT method were made using the software MSC Marc/Mentat. A simple plate model representing the peened area was constructed using first-order hexahedral elements with further mesh refinement around the area where the peening took take place. The mesh model had an area of 20mm x 20mm, a plate thickness of 5mm and a total of 1024 elements. The peening area was set to automatically refined the nearby mesh when the nodes entered the area surrounding the hammering pin. The elements peened were subdivided up to 4 times and the smallest element size of the refined mesh at the peening area was around 78μm.

The hammering pin used in HFMI/PIT treatment was modelled as a rigid body and was constructed using solid geometries. It consisted of a round cylinder with a hemispherical tip with a radius of 2mm. The pin was attached to a non-linear spring/dashpot element that was programmed to apply a consistent reaction force of 3400N [9]. This quasi-dynamic spring configuration can be considered a hybrid between the usual displacement-controlled system (DCS) and force-controlled system (FCS) used in other simulations of HFMI/PIT. Figure 3 and Figure 4 shows the FEA model used in the HFMI/PIT simulation and the graph of the nodal displacement against force of the spring function respectively.

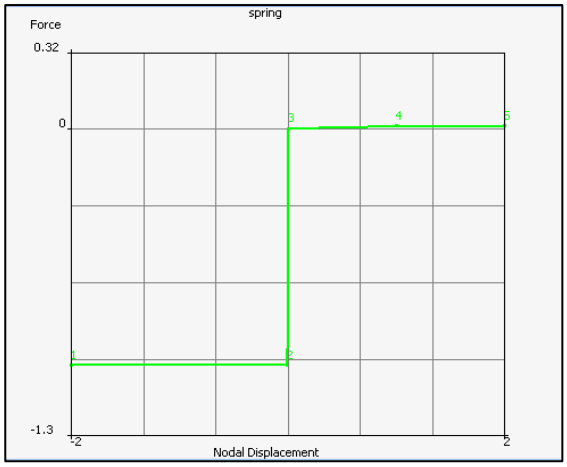

Fig. 3. FEA models used in the HFMI/PIT simulation.

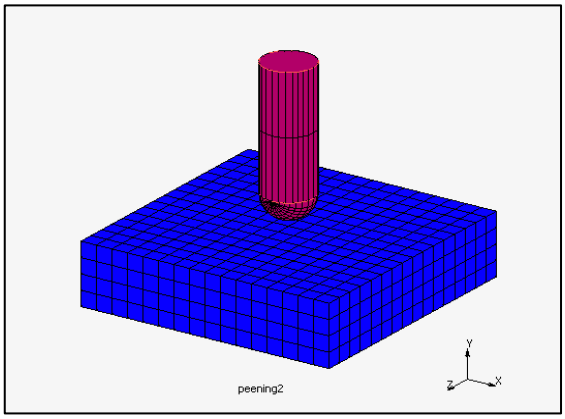

Fig. 4. Graph of the spring function parameter.

One advantage of this quasi-dynamic method has over the usual DCS and FCS approach is that the force applied to the material surface is independent of the displacement of the pin or the gap between the pin and the surface [10,11]. This allows a consistent application of the peening force regardless of the variation in gap between the pin and the surface not unlike effect of the fluidic muscle system employed by the HFMI/PIT method. Perturbation of surface nodes of a mesh model due to welding or other processes that can cause nodes displacement on the surface no longer influence the force applied by the peen. The result of this quasi-dynamic approach to simulating HFMI/PIT with 3 different gap values is shown in Table 3 and Figure 5 below:

Table 3. Effect of gap size on indentation depth.

Pin gap d_g (mm)	0.200	0.400	0.600
Indentation (mm)	0.151	0.150	0.149

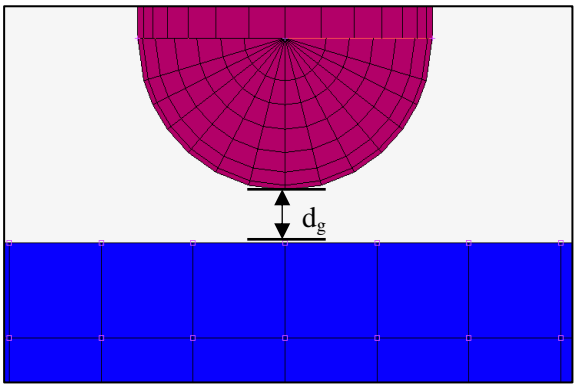

Fig. 5. Gap between the pin and the surface.

The material behaviour model of the simulation was based on the simplified Hensel-Spittel model 1 (HS1). The HS1 parameters used for the simulation was obtained from the material database software MatILDa that is used by the software MSC Simufact Forming. The HS1 constitutive equation used in the simulation is given as [12]:

$$\sigma = A.e^{m_1.T}.\varphi^{m_2}.e^{\frac{m_4}{\varphi}}.\dot{\varphi}^{m_3} \quad (10)$$

where

A is the scaling factor

T is the temperature

m_1 is the material's sensitivity to temperature

m_2 and m_4 are the material's sensitivity to strain

m_3 is the material's sensitivity to strain rate

The values of the parameters used for the HS1 model equation are as shown in Table 4 below:

Table 4. Values of the parameters used for the HS1 model

Parameter	A	m_1	m_2	m_3	m_4
Value	921.78	-0.0012	0.11291	0.0186	-0.0106
Temperature (T)	20°C – 300°C				
Strain (φ)	0.05 – 2.0				
Strain rate ($\dot{\varphi}$)	$0.01s^{-1}$ – $250.0s^{-1}$				

To account for the residual stress of the weld toe due to the welding process, a pre-stress condition was applied to the mesh plate via the initial condition parameter of the simulation. The initial stress values were obtained directly from the XRD residual stress measurements of the specimens. The initial stress applied at the beginning of the simulation was allowed to relax and settle to a stabilized value after a certain amount of time before the HFMI/PIT process started. A

settling time of 5 seconds was applied, and the residual stress values were reduced in elements near the edge of the plate, but in the middle where the peening took place the elements still maintained an acceptable value that is comparable to the initial stress input.

The longitudinal displacement of the pin followed a sinusoidal function with a frequency of 90Hz and a peak-to-peak displacement of 1mm. The gap between the pin and the surface of the mesh plate was set around 0.5mm and normal to the surface of the model. The pin was moved across the mesh plate forward and back 3 times in total, with an infeed speed of around 45 mm/s and producing 3 indentations for every pass. This resulted in an indentation overlap factor of around 1.7. Figure 6 shows the peened surface of the mesh model. Lastly, after the HFMI/PIT simulation was performed, the longitudinal and transverse residual stress values were extracted for comparison with actual measurements of the butt joint specimens.

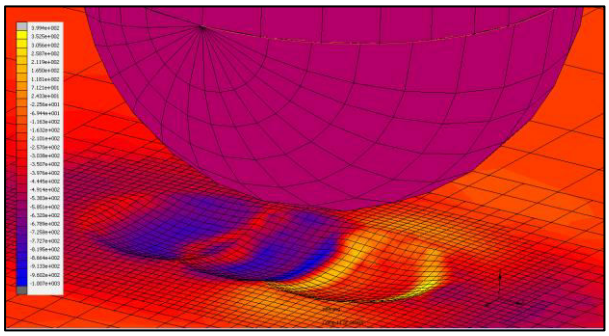

Fig. 6. Refined mesh of the peened area

5 Result of residual stress measurements

The complete result of the residual stress measurements is presented in Table 5 below. The residual stress analysis software that was used to calculate the residual stress had a predefined confidence level of 68.3% and the margin of errors were calculated based on the t-distribution function. The result shows significant margin of error values for several measurement points. There is no observable correlation in terms of margin of error due to the direction of the stress nor the before-and-after treatment with HFMI/PIT which suggests that the generalized XRD measurements parameters used were inadequate for every sample point tested.

The residual stress values were then averaged from all the measurement points and presented in Table 6 below. The result shows an increase in compressive stress between untreated and HFMI/PIT treated in both the longitudinal and transverse direction of the weld line. The averaged results show residual stress difference between the longitudinal and the transverse values of measurements points. The result shows the tendency of the welding process to develop tensile residual stress in the direction transverse to the weld line.

Table 5. Result of residual stress measurements (MPa).

		Point 1			
		Long.	Rel. (±)	Trans.	Rel. (±)
Specimen 1	Treated	-278.73	322.51	179.03	75.27
	Untreated	-80.42	56.36	212.87	24.02
		Point 2			
		Long.	Rel. (±)	Trans.	Rel. (±)
	Treated	-161.77	293.05	141.36	25.48
	Untreated	-358.98	12.26	247.65	50.69
		Point 3			
		Long.	Rel. (±)	Trans.	Rel. (±)
	Treated	18.08	87.23	-353.72	32.96
	Untreated	-290.90	19.72	-768.88	128.67
Specimen 2		Point 4			
		Long.	Rel. (±)	Trans.	Rel. (±)
	Treated	-600.50	13.13	100.38	67.82
	Untreated	-106.68	63.87	-67.72	94.52
		Point 5			
		Long.	Rel. (±)	Trans.	Rel. (±)
	Treated	-213.47	216.56	262.39	25.60
	Untreated	-93.72	94.99	244.47	154.48
		Point 6			
		Long.	Rel. (±)	Trans.	Rel. (±)
	Treated	-202.21	78.65	207.89	65.05
	Untreated	-80.23	59.47	-251.74	62.74
Remark:		*Long. - Longitudinal *Trans. - Transverse		*Rel. - Reliability (margin of error)	

Table 6. Averaged values of measurement points (MPa).

	Longitudinal		Transverse	
Point	Untreated	Treated	Untreated	Treated
1	-80.42	-278.73	179.03	212.87
2	-358.98	-161.77	141.36	247.65
3	-290.90	18.08	-353.72	-768.88
4	-106.68	-600.50	100.38	-67.72
5	-93.72	-213.47	262.39	244.47
6	-80.23	-202.21	207.89	-251.74
Average	**-168.49**	**-239.77**	**89.56**	**-63.89**
Difference		*-71.28*		*-153.45*

In the longitudinal direction, the compressive residual stress measured despite the welding process can be reasonably attributed to the residual stress of the base plate itself existing before the welding was applied. HSLA steel plates that are manufactured by thermally controlled rolling exhibits a compressive stress near the surface of the plate that might not be significantly affected or reduced by the welding process. Furthermore,

the direction of rolling process during the manufacturing of the plates produces an anisotropic stress profile along the surface of the plate. It is probable that the tensile residual stress produced by the welding process is not high enough to overwhelm the existing compressive stress in the plate especially along the direction of the weld line where the welding tensile residual stress produced is much lower than the one perpendicular to it.

6 Assessing measured and simulated values

In order to evaluate the residual stress simulated against measured values of the HFMI/PIT process, the scalar values of component 11 and 33 of the stress tensor - representing the stress along longitudinal and transverse direction of the weld line - were extracted from the simulation. The stress values were extracted from the surface nodes in and around the indentation area which amounted to between 1700 to 2457 nodes. The nodal stress values were averaged and compared with the experimental values from the XRD measurements. The result of the comparison is shown in Table 7 below:

Table 7. Comparison between experiment and simulation (MPa)

		Exp.	Sim.	Difference	Diff. (%)
Long.	Untreated	-168.49	-161.83	**6.66**	*3.95*
	Treated	-239.77	-240.96	**-1.19**	*-0.50*
Trans	Untreated	89.56	98.76	**9.20**	*10.27*
	Treated	-63.89	-222.39	**-158.50**	*-248.08*
Remark:		*Exp. – Experiment		*Sim. - Simulation	

The result shows reasonably good correlation between the experimental and simulated values of HFMI/PIT induced residual stress except for the transverse treated values which shows a large difference of almost 250%. This large discrepancy could be attributed to the way the XRD residual stress values were measured. The decision to arbitrarily measure different points and averaging them for the untreated and treated specimen points may have likely contributed to the large variations between samples within the same group of points.

The large variation between samples of the same grouping also suggest that residual stress development due to the welding process was much more localized than first anticipated. Increasing the sample size would help reduce the variation between sample values but at the expense of longer time to conduct the measurements. An XRD residual stress measurement on one sample point could take between 3 to 4 hours to finish and it would be very costly in terms of time to collect enough measurements to reduce the variation to within an acceptable limit statistically.

A better approach to could be to measure the residual stress on specified locations before and after HFMI/PIT treatment. While this would not alleviate the issue of a small sample size, it would allow for a better comparison of residual stress values between measurements of before and after the treatment. There is also the issue the surface roughness of the HFMI/PIT treated surface due to the indentations that might also cause the higher variations than is normal. Other factors that could contribute to the high variations include the development of shear residual stresses from the indentations on the surface and the visual qualitative nature of the evaluation process for HFMI/PIT.

On the simulation side, further improvements can be made to the material behavior model used in the simulation. The model used was based on the simplified Hensel-Spittel model that contained 5 terms that defined the flow curves. The use of a more accurate flow curves derived from the actual tensile, compressive or shear tests should yield a result that is closer to the measurements, but it might not be cost effective compared to existing parametric models. Another area that might be improved upon is the peening speed and overlap. The HFMI/PIT treatment process is operated manually by a human operator, and its qualification depends largely on visual qualitative inspection. Such process makes it difficult to quantify parameters such as peening speed, indentation overlap and angle of attack. Somewhat resolving such uncertainties would allow for better matching of simulation parameters with the actual process that would to better results.

The effect of overlapping the indentations in the simulation was also investigated. The stress and total strain in the longitudinal and transverse direction were extracted from the deformed surface nodes at the 1st pass and the 2nd and final pass of the peening. Table 8 below shows values and the differences between the 1st and the 2nd pass of the nodal stress and total strain. The shows an inverse relation between the stress and the total strain of the indentations as the number of peening pass was increased. The residual stress of the indentations is reduced as a second peening pass was applied but the total strain values were increased instead by a factor of around 2.

Table 8. Comparison between 1st and 2nd peening pass.

		1st pass	2nd pass	Difference	Diff. (%)
Long.	Stress (MPa)	-338.42	-240.96	**97.46**	*-28.80*
	Total Strain	0.0054	0.0089	**0.0034**	*63.28*
Trans.	Stress (MPa)	-255.32	-222.39	**32.93**	*-12.90*
	Total Strain	0.0056	0.0068	**0.0012**	*22.08*
Remark:		*Long. – Longitudinal		*Trans. – Transverse	

While further tests need to be conducted, it is reasonably expected that the stress and total strain values would converge to a stable constant as the number of peening passes increase. Experimental validation of multiple peening passes would be difficult to achieve satisfactorily in practice due to the high variation in nature of the HFMI/PIT treatment. However, such conciliation between experimental and simulated values would provide valuable information in predicting fatigue life of welded joint structures.

The authors would like to express their utmost gratitude to all the persons involved in this research. Special mention goes to Mr. Azrriq Zainul Abidin of Tecnogerma Engineering & Consulting, Dr. Mohamed Ackiel Mohamed of Serba Dinamik Holdings, Dr. Martin Leitner and Dr. Michael Stoschka of Montan University Leoben, Austria, and Dr. Marcel Graf and his team at TU Chemnitz, Germany for their valuable input on this research. This research is financially sponsored by Fundamental Research Grant Scheme (FRGS) with Reference. No. FRGS/1/2016/TK03/UITM/03/2.

References

1. J. Billingham, J. V. Sharp, J. Spurrier, P. J. Kilgallon, *Review of the performance of high strength steels used offshore - Research Report **105*** (School of Industrial and Manufacturing Science, Cranfield University, 2003).
2. K. Nishioka, K. Ichikawa, Progress in thermomechanical control of steel plates and their commercialization, *Science and Technology of Advanced Materials*, vol. **13**, no. **2** (Apr. 2012).
3. https://masteel.co.uk/2017/01/31/s460g2qm/. Accessed on 4 Jan 2018.
4. S. Jindal, R. Chhibber, N. Mehta, Issues in welding of HSLA steels, *Advanced Materials Research*, vol. **365**, pp. 44-49 (Switzerland: Trans Tech Publications, 2012)
5. R. W. Warke, W. A. Bruce, D. J. Connell, S. R. Harris, M. Kuo, S. J. Norton, Carbon and Low-Alloy Steels, *Welding Handbook (9th Edition),* vol. **4**, A. O'Brien, C. Guzman, Eds. (American Welding Society, 2004)
6. G.B. Marquis, Z. Barsoum, IIW Recommendations for the HFMI Treatment: For Improving the Fatigue Strength of Welded Joints. Singapore: (International Institute of Welding, 2016)
7. PITEC GmbH. PIT Short Presentation. https://www.pitec-gmbh.com/application/files/8214/8173/3451/2016-12-14_17-37_998.pdf. Accessed on 28 Mar 2018.
8. R. Bjørhovde, J. Brozzetti, G. A. Alpsten, L. Tall, Residual Stresses in Thick Welded Plates, *Welding Journal (Welding Research Supplement),* pp. 392-405 (Aug 1972)
9. J. Foehrenbach, V. Hardenacke, M. Farajian, High frequency mechanical impact treatment (HFMI) for the fatigue improvement: numerical and experimental investigations to describe the condition in the surface layer, *Welding in the World*, vol. **60**, no. **4** (July 2016)
10. D. Simunek, M. Leitner, and M. Stoschka, Numerical simulation loop to investigate the local fatigue behaviour of welded and HFMI-treated joints (IIW Commission XIII Fatigue Of Welded Components And Structures XIII-WG2-136-13)
11. R. Baptista, V. Infante, C. Branco, Fully Dynamic Numerical Simulation of the Hammer Peening Fatigue Life Improvement Technique, *Procedia Engineering*, vol. **10** (2011)
12. M. di Donato, Flow curve determination by torsion tests using inverse modelling, *Master's Degree Dissertation*, (Department of Mechanical Engineering, University of Padova, 2016)